

Finding pulsars with LOFAR

Joeri van Leeuwen¹ and Ben Stappers²

¹ Stichting ASTRON, PO Box 2, 7990 AA Dwingeloo, The Netherlands, leeuwen@astron.nl

² Jodrell Bank Centre for Astrophysics, School of Physics and Astronomy, University of Manchester, Manchester M13 9PL, UK

Received / Accepted

ABSTRACT

We investigate the number and type of pulsars that will be discovered with the low-frequency radio telescope LOFAR. We consider different search strategies for the Galaxy, for globular clusters and for other galaxies. We show that a 25-day all-sky Galactic survey can find approximately 900 new pulsars, probing the local pulsar population to a deep luminosity limit. For targets of smaller angular size such as globular clusters and galaxies many LOFAR stations can be combined coherently, to make use of the full sensitivity. Searches of nearby northern-sky globular clusters can find new low luminosity millisecond pulsars. Giant pulses from Crab-like extragalactic pulsars can be detected out to over a Mpc.

Key words. pulsars: general — telescopes — surveys

1. Introduction

Since the discovery of the first four pulsars with the Cambridge radio telescope (Hewish et al. 1968), an ongoing evolution of telescope systems has doubled the number of known radio pulsars roughly every 4 years: An evolution from a large flat receiver with a fixed beam on the sky (the original Cambridge radio telescope) to focusing dishes (Arecibo – Hulse & Taylor 1975), often steerable (Green Bank Telescope), on both hemispheres (the Parkes telescope – Manchester et al. 2001), with large bandwidths and multiple simultaneously usable receivers for wider fields of view (Parkes, Arecibo). The types of pulsars discovered have changed accordingly, from slow, bright, single and nearby pulsars (the original four) to fast (young and millisecond pulsars), far-away (globular clusters) or dim pulsars, some of which are in binaries.

The next step in radio telescope evolution will be the use of large numbers of low-cost receivers that are combined interferometrically. These telescopes, the Allen Telescope Array (Bower 2007), LOFAR (Röttgering 2003), MeerKAT (Jonas 2007), ASKAP (Johnston et al. 2008) and the SKA (Kramer 2003), create new possibilities for pulsar research.

In this paper, we investigate the prospects of finding radio pulsars with LOFAR, the LOw Frequency ARray. We outline and compare strategies for targeting normal and millisecond pulsars (MSPs), both in the disk and globular clusters of our Galaxy, and in other galaxies.

2. LOFAR - The LOw Frequency ARray

With the first test station operational and the first pulsars detected LOFAR is on track to start operation in 2010. We have evaluated and simulated the LOFAR reference configuration for pulsar searches, and will describe that configuration in some detail below.

Using two different types of dipoles, LOFAR can observe in a low and a high band that range from 30-80 MHz and 110-240 MHz respectively. The sensitivity using the high-band antenna (HBA) is several times that of the low-band antenna (LBA)

although their survey speeds are similar due to the larger LBA field of view. The low band is expected to be an exciting new window for exploring radio pulsar behavior (cf. Stappers et al. 2007, for an overview of the possibilities for emission physics and interstellar medium studies), but the impact on a pulsar survey of some of the smearing effects further discussed is so strong in the LBA band, that we will only discuss the HBA half of LOFAR in this paper.

The basic collecting elements are the individual dual-polarization dipoles; each 4x4 set of these dipoles is combined in an analog beamformer and forms an antenna 'tile'. Tiles are grouped together in stations; stations farther from the array center are larger than inner stations. In the core, HBA stations are grouped in pairs. The innermost 12 stations are 24 tiles each and are packed tightly in a 'superstation'. Spread over the 2-km core there are 24 more HBA stations of 24 tiles each (making for 36 core stations in total). These core stations are 32 meters in diameter, but are tapered to an about 30 meter effective diameter to reduce sidelobes. Next there are 18 Dutch 'remote' stations that are outside the core and consist of 48 tiles each, while the ~8 international stations that are spread over Europe use 96 HBA tiles.

At each station the tiles are combined to form up to 8 independently steerable 'station beams'. With the cumulative data rate out of the station being the limiting factor, the product of the number of beams times their bandwidth cannot exceed 32 MHz (potentially 48 MHz), e.g.: a station beam set up can range from having a single full-bandwidth station beam to 8 independent beams of 4 MHz each. Station beams are subdivided in 195 kHz channels, and sent to the central processor (CEP) supercomputer for correlation, addition and/or different types of beam forming. As illustrated in Fig. 1 CEP can further combine station beams to form ~128 16-bit full-polarisation tied-array beams for the superstation, the core and/or the entire array. That number of formed beams is limited by the maximum CEP output rate, currently 50 Gigabits/second.

The high-band antennas operate in a 110–240 MHz frequency range and are spaced to optimize sensitivity for the low end. They are maximally sensitive toward the zenith. The fall-

off of effective area A_{eff} with zenith angle and observing frequency has been well characterized as shown in Fig. 2 (after Wilhelmsson 2007) and we will also describe it qualitatively here: at its maximum at 120 MHz, the effective area toward zenith is 28 m^2 per antenna tile, halving at a zenith angle of $\sim 50^\circ$. Toward higher frequencies both quantities decrease until at 240 MHz the maximum effective area is 8 m^2 per antenna tile, dropping to half that at $\sim 30^\circ$ away from zenith. For the $N_{station} = 36$ stations of the compact core at 120 MHz, with their $N_{tiles} = 24$ tiles each, this effective area translates into a theoretical maximum core gain $G_{max,core}$ of

$$G_{max,core} = \frac{28 \text{ m}^2 N_{stations} N_{tiles}}{2k} \times 10^{-26} \frac{\text{W s}}{\text{Jy m}^2} = 8.8 \text{ K/Jy} \quad (1)$$

where k is Boltzmann's constant in W s m^2 . Finally, the noise temperature $T_{antenna}$ of the HBA is expected to be 140 K at 120 MHz and around 180 K in the upper half of the band (Gunst 2007).

3. Pulsar searches

3.1. All-sky surveys

Although a pulsar survey generally addresses several science questions in parallel, it can be optimized for a specific goal: by using short integration times potential acceleration smearing is kept to a minimum to optimize for finding millisecond pulsars; when aiming to maximise the total number of new pulsars found, a survey should generally focus on the Galactic plane; while for a representative understanding of the local population an all-sky survey that is equally sensitive in all directions is optimal. Here we will focus on such an all-sky survey.

Below we first investigate different beam forming scenarios. These we compare assuming use of a single station beam, at full bandwidth, at the lowest observing frequency of 120 MHz. We investigate frequency and band width dependencies in more detail in subsection 3.1.2.

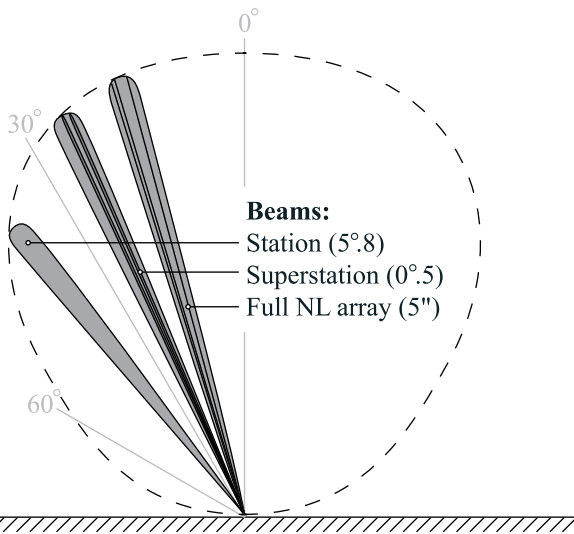


Fig. 1. Illustration of station, superstation and full-array beam patterns at 120 MHz. The zenith is at 0° . The dashed envelope is the tile response as shown in Fig. 2. The gains of the different beams are here scaled to be the same. Three stations beams are shown, up to eight can be formed at a given time.

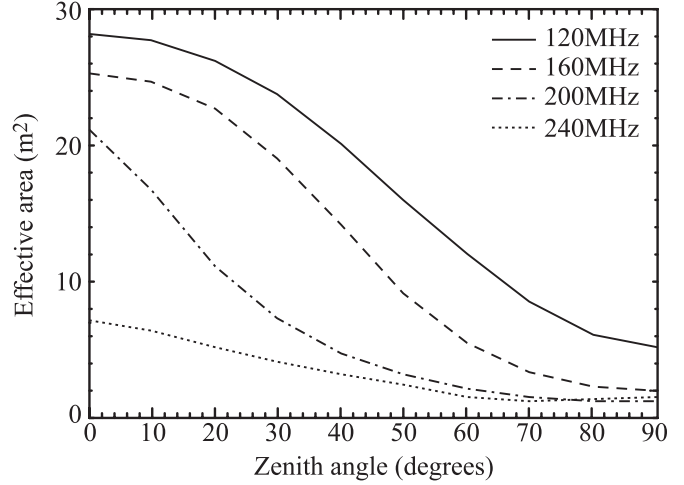


Fig. 2. Simulated effective area per antenna tile versus zenith angle, for 4 different observing frequencies. From Wilhelmsson (2007).

3.1.1. Beam forming

To first order an all-sky pulsar survey is optimized to reach best sensitivity per given overall time. For that one should minimise system noise while maximising collecting area, bandwidth, and integration time per pointing.

For a given survey time and sky area, maximising the time per pointing is equivalent to maximising the instantaneous field of view. This can be done by forming multiple simultaneous beams; while for sparse telescopes like LOFAR, where receivers are spread out over a large area, one can also add stations incoherently instead of coherently. This increases the field of view at the cost of increasing uncorrelated noise over correlated signal (cf. Backer 1999). In the incoherent case the beam on the sky will be larger, but in the coherent case the system is more sensitive.

From the above we can construct the following survey figure of merit FoM for a given observing frequency (see Cordes 2002; Smits et al. 2009, for related definitions):

$$FoM = 10^{-3} \left(\frac{A}{T_{sys}} \right) \left(\frac{N_{beams} \Omega B}{1|N_{stations}|} \right)^{1/2} \quad (2)$$

where the factor 10^{-3} scales the reference FoM to be 1.0; A/T_{sys} is the ratio of effective area and system noise equivalent temperature, averaged over the field of view, a ratio indicating telescope gain. N_{beams} is the number of simultaneous beams formed and Ω denotes the field of view as derived from the beam size. Here and below we estimate all beam sizes by their full width at half maximum (FWHM) as $1.22 \frac{\lambda}{D} \frac{360}{2\pi}$ deg with λ the observing wavelength, and D the diameter of the element over which the beam is formed (e.g.: a station, the core, or the full array). Then $\Omega = \pi \left(\frac{FWHM}{2} \right)^2 \text{ deg}^2$. B is the observing bandwidth; the right-hand denominator is 1 for coherent addition, or $N_{stations}$ when that number of stations is added incoherently. This FoM is inversely proportional to the minimum detectable flux S_{min} . When comparing between setups, the ratio of survey speeds – the time needed to reach a given sensitivity over the whole sky – is FoM^2 . In Table 1 we list the FoM for three survey set ups discussed below.

To outline the various trade-offs involved with these survey setups, we first compare scenarios for coherent versus incoherent addition for the LOFAR core only, and not the total array – given

Type	A/T_{sys} (m ² /K)	N_{beams}	Ω (deg ²)	B (MHz)	$1/N_{\text{stations}}$	FoM
Full Incoherent	260	1	27	32	54	1.0
Core Coherent	170	128	0.006	32	1	0.8
Superstation Coherent	40	128	0.23	32	1	1.2

Table 1. Figure of merit FoM per Eq. 2 for the three different survey set ups as described in the text: Full Incoherent, Core Coherent and Superstation Coherent. All parameters derived using the lowest observing frequency, 120 MHz. In the first column, A/T_{sys} , we use 54, 36 and 12 stations respectively, of 24 tiles at 28 m², and 140 K, while for the *Superstation Coherent* case we also multiply by 0.70 to correct for the lower sensitivity at the station beam edge.

the sparseness of the distribution of remote stations, coherent addition of the entire array would result in an extremely limited field of view.

In the *Core Coherent* scenario all 36 stations in the 2 km diameter D_{core} compact core are combined coherently. In this case $\Omega = 0.0060 \text{ deg}^2$ and the gain is as per Eq. 1. For comparison, each of the individual roughly $D_{\text{station}} = 30\text{-meter}$ core stations forms a beam on the sky of 27 deg^2 . If added incoherently, the resulting beam is as large as for an individual core station (cf. Fig. 1) but at a factor $\sqrt{N_{\text{stations}}} = 6$ decreased sensitivity compared to the coherent case. The factor $(\frac{D_{\text{core}}}{D_{\text{station}}})^2 = (\frac{2000\text{m}}{30\text{m}})^2 = 4.4 \times 10^3$ increase in beam area allows for longer integrations by the same factor. For synthesis telescopes that form a single coherent ‘tied-array’ beam, like the Westerbork Synthesis Radio Telescope or the Very Large Array, such a factor would well describe the trade-off; but as the LOFAR CEP can output $N_{\text{beams}} = \sim 128$ coherently added core beams simultaneously versus only a single incoherently added core beam, the factor F_t difference in integration times is $F_t = (\frac{D_{\text{core}}}{D_{\text{station}}})^2 / N_{\text{beams}} = (\frac{2000\text{m}}{30\text{m}})^2 / 128 = 35$. Thus, in this comparison the sensitivity decrease by $\sqrt{N_{\text{stations}}} = \sqrt{36}$ of adding stations *incoherently* and the sensitivity increase by $\sqrt{F_t} = \sqrt{35}$ provided by longer integrations practically cancel out: the FoM for coherent or incoherent addition of just the core is very similar.

Although for the *coherent* sum the addition of remote stations significantly reduces the field of view, for the incoherent case the entire array can be added without field-of-view penalty. Physically the remote stations are twice the size of the core stations but they can be tapered to the size of the core stations to produce a similar field of view. Adding these 18 remote stations in the above equation produces a FoM for the *Full Incoherent* scenario of 1.0; that is $(F_t N_{\text{stations,full}})^{1/2} / N_{\text{stations,core}} = (35 \times 54)^{1/2} / 36 = 1.2$ times higher than FoM for the *Coherent Core* case which is 0.8 (Table 1). Yet (only) for the *Coherent Core* survey producing more simultaneous beams increases the FoM; if 50% more beams could be formed these two scenarios would be equally sensitive.

Incoherent addition may offer slightly better sensitivity because it allows for long integration times. If however these long integration times are a significant part of a potential pulsar binary orbit (cf. 1-hr integrations in our reference incoherent survey, defined below, versus the 2.4-hr binary period of PSR J0737-3039 Burgay et al. 2003), the apparent change in pulse period due to the acceleration through the orbit decreases the effectiveness of periodicity searches. At a computational cost different types of acceleration searches can mitigate this decrease in sensitivity (Johnston & Kulkarni 1991; Ransom et al. 2003). A coherent survey is less prone to this acceleration smearing: to reach the same S_{min} as the incoherent reference survey with 1-hr pointings, the coherent addition survey integration time is down to 3 minutes. From an efficiency point of view short pointings are also more robust to system errors such as data glitches, and

to impulsive radio interference. In contrast to searching a single beam for an incoherent-addition survey, handling ~ 128 simultaneous data streams, each at high time resolution and totaling 50 Gigabits/second is a significant computational and data-handling task (Backer 1999; cf. Smits et al. 2009 for the SKA).

In a different coherent survey, *Superstation Coherent*, 128 tied-array beams from just the superstation (cf. section 2) tile out the complete station beam. Compared to coherently adding the entire core, the superstation beams have larger field of view but are less sensitive. In a grid of 128 of these wider superstation beams many will be close to the less sensitive edges of the station beam, causing for some decrease in sensitivity compared to the narrow *Coherent Core* beams. For A/T_{sys} in Table 1 we hence use the average sensitivity out to FWHM for an assumed Gaussian station beam, which is 70% of the sensitivity for the center of the beam. Yet the relatively large field of view caused by the dense packing of the superstation offsets the limited sensitivity of the lower number of stations now used, producing a FoM of 1.2, compared to 1.0 for the incoherent survey discussed above. Given identical overall survey duration, the integration times for this coherent superstation and the incoherent full array are similar, so there is no reduction in acceleration smearing. Inherent to coherent-addition surveys, the computational task of searching through 128 beams simultaneously and in real-time remains.

Beam forming scenarios have an impact on how accurately sources can be located; this we will address in more detail in section 4 where we discuss follow up.

3.1.2. Observing frequency

Determining the optimum observing frequency involves mapping out the trade-off between beam size, source and background brightness, and pulse smearing from dispersion and scattering. Some telescope and pulsar behavior favors low-frequency observing: when moving up from the lowest frequencies the beam size decreases as ν^{-2} which limits integration time per pointing in a fixed-time all-sky survey; the effective collecting area falls off with frequency; and the intrinsic pulsar brightness decreases with frequency as $\nu^{-1.5}$ on average (Malofeev et al. 2000). Other circumstances are more favorable at higher frequencies: the background sky noise decreases steeply as $\nu^{-2.6}$ (Lawson et al. 1987) and smearing from interstellar dispersion and scattering, which makes the pulsar periodicity harder to detect, is less. Much of the effect of dispersion can be removed by searching over many ($\sim 10^4$) incoherently dedispersed trial DMs (Lorimer & Kramer 2005). No such removal process exists for scatter broadening, where the pulsar emission takes different paths through the interstellar medium with different travel times, resulting in an observed pulse profile that is significantly smeared out. Scattering smearing time increases sharply with decreasing observing frequency (as $\nu^{-4.5}$, Ramachandran et al.

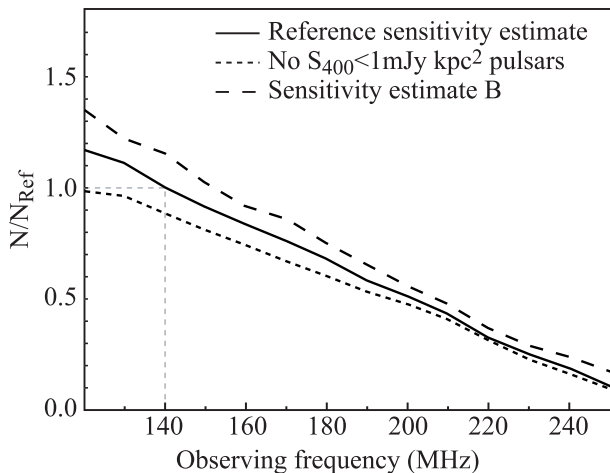


Fig. 3. Number of pulsars detected in simulated surveys at different frequencies and sensitivity estimates, plotted as a ratio over the productivity of our reference 25-day all-sky survey of 1-hr pointings at 140 MHz. Towards lower frequencies the yield goes up, mostly caused by the increasing effective area as the wavelength approaches the telescope’s optimum at twice the antenna spacing of 1.25 m; equally important is the increasing beam size which allows for longer integrations for the same total survey time.

1997; or alternatively $\nu^{-3.9}$, Bhat et al. 2004) and with increasing distance to the pulsar (Taylor & Cordes 1993).

Although the sky background and scatter broadening increase towards lower frequency we find in our simulations, further described below, that the total survey productivity, if defined as the total number of pulsars detected (Fig. 3), is mainly determined by the effective collecting area and the beam size. These peak towards the lower edge of the band, leading us to conclude that the survey is most efficient at lowest frequencies. When using a single full-bandwidth 32 MHz station beam this means a central frequency of 140 MHz, from here on our reference frequency. As can be seen from Eq. 2, bandwidth can be freely traded for beams with no impact on the FoM. Splitting up the available bandwidth over multiple independently pointing stations beams (keeping beams-bandwidth product equal to 32 MHz as outlined in Section 2) and moving each beam to a lower, more sensitive observing frequency may therefore further increase the overall survey output. This does increase integration time per pointing, which may be only beneficial in the *Core Coherent* scenario where short default integration times could limit sensitivity to intermittent pulsars.

3.1.3. Sensitivity

The minimum detectable flux S_{min} depends on the signal-to-noise ratio at which one accepts a signal as real (SNR), the system temperature ($T_{sys}=T_{rec}+T_{sky}$) as it varies over the sky, the number of polarisations (N_{pol}), the bandwidth (B), the integration time (t), the pulsar period (P) and pulse width (W) and the zenith-angle dependent gain $G(z)$. Compared to the theoretical gain the real-life gain is always less; although in Eq. 1 we already use the simulated *effective* area and take aperture efficiency into account there, we apply a conservative factor 0.66 to estimate the real-life gain for our simulations below. Regarding the impact of RFI on the amount of usable bandwidth, testing has shown the radio-interference environment to be relatively

clear, and RFI is significantly reduced by the 12-bit digitisation and the many-element interferometer design, especially when elements are combined coherently. As the total bandwidth can furthermore be quickly split up and spaced to avoid channels contaminated by RFI, we expect that the entire specified 32 MHz band (potentially 48 MHz) will be usable, but below we shall conservatively use 80% of 32 MHz. The potential 1.5-fold increase in usable bandwidth from 32 to 48 MHz would increase sensitivity by $\sqrt{48/32}$. As S_{min} depends on zenith distance and sky noise it varies per pointing, but after Dewey et al. (1985) we can estimate a typical value for a 1-minute pointing towards the zenith using a coherently formed core beam, for a pulsar with a 10% duty cycle:

$$\begin{aligned}
 S_{min} &= SNR \left(\frac{T_{sys}}{0.66 G_{max} (N_{pol} 0.8 B t)^{\frac{1}{2}}} \right) \left(\frac{W}{P - W} \right)^{\frac{1}{2}} \\
 &= 10 \left(\frac{1.0 \times 10^3 \text{ K}}{0.66 \times 8.8 \frac{\text{K}}{\text{Jy}} (2 \times 0.8 \times 32 \text{ MHz} \times 60 \text{ s})^{\frac{1}{2}}} \right) \left(\frac{1}{3} \right) \\
 &= 10.3 \text{ mJy}
 \end{aligned} \tag{3}$$

For comparison the S_{min} for incoherently added pointings for our reference survey described below (1-hr integrations, 54 stations added) comes to 5.8 mJy.

3.1.4. Simulations

To determine the number and type of pulsars LOFAR can find, we have used the above characteristics to model the detection of a large number of simulated normal pulsars. For this, we have used a population synthesis code that simulates the birth, evolution, death and possible detection of radio pulsars (for details see Bhattacharya et al. 1992; Hartman et al. 1997; van Leeuwen & Verbut 2004). We do not simulate *millisecond* pulsars, as a realistic treatment of the survey selection effects associated with their binary history would be essential but is beyond the scope of this work. For our simulated pulsars we draw birth velocities from the Lyne & Lorimer (1994) distribution with its $450 \pm 90 \text{ km s}^{-1}$ mean velocity. Initial positions are simulated as in Hartman et al. (1997): heights above the Galactic

Survey	Year	N_{real}	N_{sim}	ν (MHz)
Jodrell	1972	51	20 ± 2	408
UMass-Arecibo	1974	50	39 ± 4	430
MolongloII	1978	224	227 ± 7	408
UMass-NRAO	1978	50	54 ± 6	400
ParkesII	1991-1994	298	335 ± 10	400
Cambridge 80MHz	1993-1994	20	27 ± 5	82
Parkes Multibeam	1997-2000	987	801 ± 41	1374
LOFAR	2010-2012	–	1100 ± 100	140

Table 2. Name, year, number of detected pulsars (N_{real}), number of simulated detected pulsars (N_{sim}) and frequency observed at (ν) for the eight surveys simulated. The error on N_{sim} is the standard variation in the outcomes when simulating the model described in the text with different random number seeds. The N_{real} data is taken from Davies et al. (1977); Hulse & Taylor (1975); Manchester et al. (1978); Damashek et al. (1978); Manchester et al. (1996); Shrauner et al. (1998) and Manchester et al. (2005) respectively. The LOFAR numbers are for the incoherent 25-day reference design described in the text.

plane are randomly selected from an exponential distribution with a scale height of 60 pc; for the initial distribution in galactocentric radius we use their Eq. 4, modified to scale *per unit area*:

$$p(R) dR = \frac{R}{R_w} \exp\left(-\frac{R}{R_w}\right) dR \quad (4)$$

where scale length R_w is 5 kpc. This modified distribution does not peak as strongly toward the Galactic centre; for the local population there is no significant change but surveys that sample the inner Galaxy are better reproduced. We next calculate the 3D orbits through the Galaxy. We evolve magnetic fields and periods, determine whether the pulsar is still above the death-line. We estimate the luminosity at 400 MHz (per Hartman et al. 1997, who follow Narayan & Ostriker 1990). With a spectral index drawn from a Gaussian distribution of width 0.76 around -1.5 (Malofeev et al. 2000, takes luminosity turn-overs into account) we scale this luminosity to the observing frequency.

Using the simulated position we look up the sky background temperature (Haslam et al. 1982) and combined with the distance we also estimate the dispersion measure and the scatter broadening from Taylor & Cordes (1993). Given that both sky background and scatter broadening time increase toward lower observing frequencies we next scale these using power laws with spectral index -2.6 and -4.4 respectively (Lawson et al. 1987; Taylor & Cordes 1993).

For each of the 8 pulsar surveys in Table 2 we model the sensitivity function versus period, dispersion and scattering smearing, and sky position. We also model the decrease of pulse width and hence detectability with period. By comparing the simulated and real pulsar samples for the first four of the above surveys Hartman et al. (1997) determined the most probable underlying initial model parameters.

We use this best model to determine the yield of a future survey with LOFAR. As tests, we also model the second 81.5-MHz Cambridge survey (Shrauner et al. 1998) to check the validity of our extrapolations to lower frequencies and the Parkes Multibeam pulsar survey (Manchester et al. 2001; Lorimer et al. 2006, hereafter PMB) because of its superior statistics. These tests we describe in some more detail in the two paragraphs below.

For each simulated pulsar, we model if it would be detected by the Cambridge survey given its sky position, dispersion and scatter smearing, and luminosity. We estimate the minimum detectable flux from the S_{min} versus DM and period plot in Shrauner et al. (1998), their Fig. 3. That figure does not take scattering into account, although for these simulations one realistically should. For each simulated pulsar we therefore determine the 'effective' (higher) DM-value that would produce the same smearing as the actual dispersion and scattering do combined. We next determine the sensitivity for the period and that 'effective' DM. The sensitivity thus estimated is valid for the survey's median sky background noise of 2 Jy, so we next scale it using the actual sky noise for the position of the simulated pulsar. Finally we multiply the sensitivity by the declination-dependent power response (Fig 1a., Shrauner et al. 1998) for the sky position and check if the simulated pulsar is bright enough to be detected. With 27 ± 5 simulated pulsars found, our model reproduces the actual tally of 20 pulsars quite well, validating the luminosity, sky-noise and scattering extrapolations to lower frequencies that we also use for the LOFAR predictions.

As a further check on our model, the PMB simulations find 800 ± 40 pulsars, which compares reasonably well to the actual

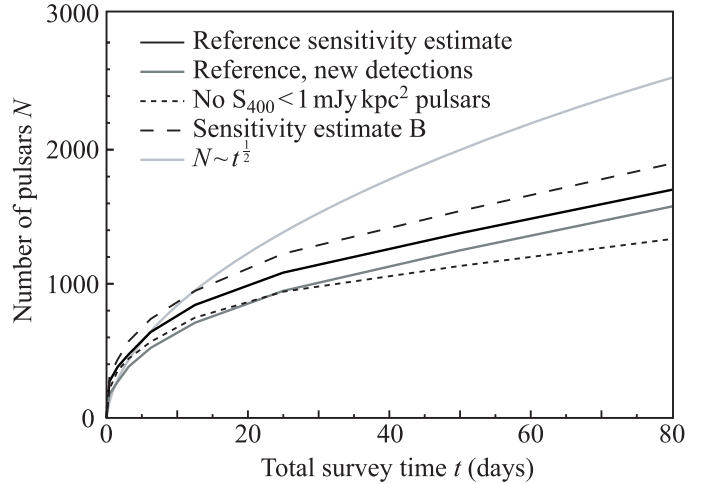


Fig. 4. Simulated number of pulsars detected in an all-sky survey, versus total survey time in days. A survey time of 25 days corresponds to 1-hr pointings for incoherently added stations beams.

number of 987 non-recycled pulsars detected (Manchester et al. 2005, ATNF catalog per Jan 1, 2009).

For LOFAR, we have evaluated surveys for different telescope parameters, total survey time and minimum sensitivity. Our reference survey is a *Full Incoherent* survey using 54 stations, 64-minute pointings, a gain per Eq. 3 of 0.66 times the theoretical gain, with 80% of 32MHz bandwidth at a central frequency of 140 MHz. With a single beam such a survey can scan the visible sky in 25 days. In an all-sky survey with this reference set up 1100 ± 100 pulsars could be detected (the full curve in Fig. 4), 900 ± 100 of which are new. Our sensitivity estimate B uses a less conservative sensitivity of 0.8 times the theoretical gain. In the same overall time it finds about 100-200 more pulsars that are new; i.e. not detected by older surveys we simulate. We do not take into account findings from ongoing surveys such as the GBT350 search project (Hessels et al. 2007; Archibald et al. 2009). Here, and below, the errors quoted for simulation runs indicate variations in output caused by using different initial random seeds. Between simulation runs, the number of new detections is a stable fraction of the total number of detected pulsars, indicating that in the simulations there is a well-defined part of the pulsar population that only LOFAR is sensitive too. In contrast, there are also known pulsars that LOFAR will not be able to detect in this reference survey, mainly due to scattering effects. We have also evaluated pointings of 1,2,4–256 minutes duration (see Fig. 4). Here the duration effects the minimum detectable flux; using the figures of merit in Table 1 this incoherent survey can be scaled to the other survey types.

If pulsar luminosity is the limiting factor in the detections, a larger time per pointing t decreases the minimum detectable flux S_{min} as $t^{-\frac{1}{2}}$, increasing the distance d out to which pulsars can be detected as $t^{\frac{1}{4}}$. At the scale of the Galaxy pulsars are located in a disk; if one could observe pulsars throughout the Galaxy, the number of detectable pulsars is $N \sim d^2 \sim t^{\frac{1}{2}}$. Locally, pulsars are distributed roughly isotropically; then $N \sim d^3 \sim t^{\frac{3}{4}}$ (cf. Cordes 2002). We find that for LOFAR surveys, N is even less dependent on t than $N \sim t^{\frac{1}{2}}$ because scatter broadening is the limiting factor,

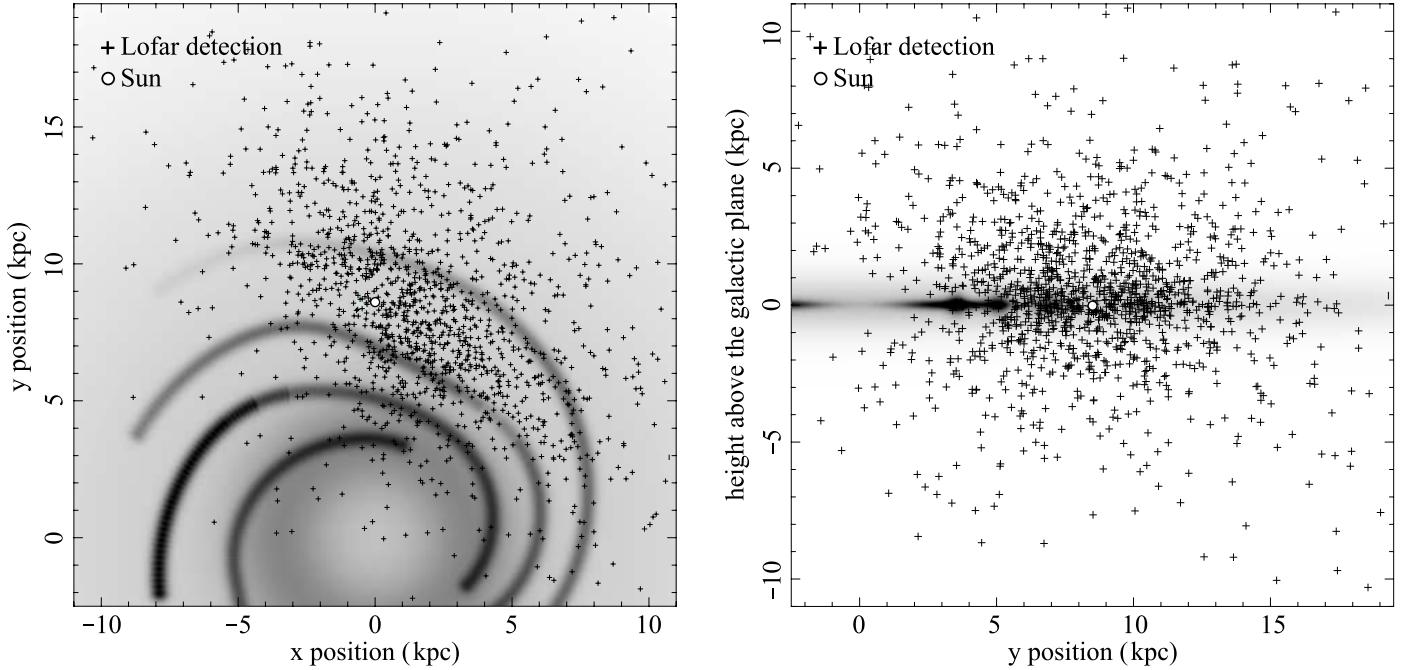


Fig. 5. The 1100 simulated pulsars detected with the reference Galactic LOFAR survey, for 1-hour pointings. The scattering interstellar matter (ISM) is shown in gray. **Left**) projected on the Galactic plane. **Right**) projected on the plane through the Galactic centre and sun, perpendicular to the disk. The Galactic centre is at (0,0,0). LOFAR probes the local population very well, while the broadening from multi-path scattering on the ISM limits what volume a low-frequency survey like LOFAR probes. (ISM modeled after Taylor & Cordes 1993).

not luminosity (cf. Fig. 4, where the $t^{\frac{1}{2}}$ line is scaled to be equal to the reference sensitivity estimate at the 6.25 day point).

Compared to the Parkes Multibeam survey, the pulsars found with LOFAR are different in several ways. The PMB is more strongly focused on the Galactic centre. The range of the population detected by LOFAR is limited by scatter broadening. Because of its higher sensitivity, LOFAR detects more low-luminosity nearby pulsars (Fig. 5a). A lower limit to pulsar luminosity of 1 mJy kpc^2 at 400 MHz has been suggested (Lyne et al. 1998, cf. similar lower limit at 1400 MHz in Lorimer et al. 2006); with a spectral index of -1.5 , this compares to a luminosity at 120 MHz of 6 mJy kpc^2 . If this lower limit exists the reference survey can detect all pulsars that are beamed toward us up to 1 kpc. If it does not exist, then this survey will certainly illuminate how many low-luminosity pulsars were formed nearby (cf. PSR J0240+62 in Hessels et al. 2007): a number of importance if one wants to understand the neutron-star birthrate.

Furthermore, LOFAR finds more pulsars out of the Galactic disk (Fig. 5b) as its high sensitivity is unimpeded by scattering in that direction. As pulsars are born in the plane ($z=0$), this observed z -distribution could disclose their much debated birth velocity (cf. Hartman 1997; Arzoumanian et al. 2002).

For the detection of millisecond pulsars (MSPs) scatter broadening will be the limiting factor. Although there is much variation in scattering measure for different lines of sight, on average the scatter broadening at 120 MHz is on the order of 1 ms for sources with DMs higher than 30 pc/cm^3 (using the rough empirical $t_{sc} = 2 \times 10^9 \text{ DM}^{3.8}$ relation between DM and scattering time by Shitov 1994) or distances of about 1 kpc (using distance-scattering relation from Taylor & Cordes 1993). As many of the currently known Galactic-disk MSPs are within this range of 1 kpc in which scatter broadening does not hinder detection (Manchester et al. 2005), LOFAR could probe the local population to a much lower flux limit.

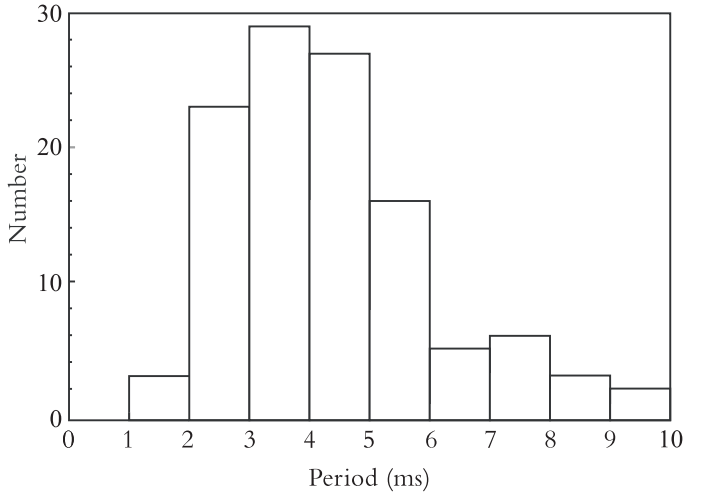


Fig. 6. Periods of the 115 MSPs in globular clusters with periods less than 10 ms. There are another 23 pulsars with longer periods. (Freire 2008).

3.2. Galactic globular cluster surveys

In a fixed-time all-sky survey, one can gain field of view at a cost of instantaneous sensitivity by adding the signal of the stations incoherently instead of coherently. When the incoherent FoM is higher (as in Table 1) this trade-off increases the number of detectable pulsars because it allows for more time per pointing. In contrast, specific, smaller regions on the sky with higher densities of radio pulsars can potentially be better targeted with smaller field of view, but significantly higher sensitivity.

Globular clusters fit the description well; they are compact and form regions on the sky with high stellar densities. These

high densities also cause globular clusters to contain more binaries and binary products than are found in the disk. This makes globular clusters very good candidates for MSP searches (e.g. Lyne et al. 1987). To estimate which clusters are most promising for a LOFAR search, we evaluated several of their properties: location on the sky, dispersion measure (DM), distance (d), and the number of radio pulsars potentially present.

As discussed above for sources in the Galactic plane, scatter broadening is a concern for detecting far-away fast millisecond pulsars. Most globular cluster pulsars have periods of around 2–5 ms (Freire 2008, see Fig. 6). Using the above mentioned DM versus scattering time relations, at 120 MHz such MSPs are detectable up to a DM of about 30–40 pc/cm³. Observing at 200 MHz extends this limit to 60–80 pc/cm³. For the longer period pulsars also present in these clusters, these limits are less of a problem, so we will further investigate globular clusters with DMs up to 100 pc/cm³ below. From studies with the Westerbork telescope Stappers et al. (2008) also conclude that the DM versus scattering time relation is uncertain to the extent that some $DM = 100$ pc/cm³ MSPs may be detectable. We rate the candidate clusters by the expected number of detectable pulsars: assuming $\frac{d \log N}{d \log L} = -1$ (Anderson 1992), this number scales as d^{-2} , as the declination-dependent telescope gain $G(z)$ (cf. Figure 2), and as the collision number $\Gamma \equiv \rho_c^{3/2} r_c^2$, where ρ_c and r_c are the central density and the core radius, respectively (Verbunt 2003). The sources that are most promising according to this scaling are listed in Table 3. The half-mass radius of each fits within a LOFAR coherent core beam (cf. Fig. 7 for highest-ranking candidate M15), which means we can now use the full gain of the coherent addition.

In general, searching globular clusters more deeply than done previously requires integrating for several hours and analyzing the data with multiple binary-acceleration search techniques (see Ransom et al. 2005, and references therein). Assuming an MSP spectral index of -1.7 (Kramer et al. 1998) the weakest pulsar in M15 (B2127+11G, 0.13 mJy at 430 MHz, from Anderson 1992) is 1.1 mJy at 140 MHz; in a 10-hour pointing with the compact core at 140 MHz, the minimum detectable flux (eq. 3 at M15’s zenith angle of 40°) is 0.5 mJy. Thus far, the luminosities of the pulsars in M15 follow $\frac{d \log N}{d \log L} = -1$. If this relation extends to lower luminosities, observing up to a minimum flux of 0.5 mJy could yield several new MSPs.

Name	DEC deg	d kpc	DM pc/cm ³	r_c arcmin	Γ	N
M15	+12	10.3	67.3	0.07	665	8
M92	+43	8.2	29 ⁺	0.23	106	
M5	+02	7.5	30.0	0.42	79	5
M10	-04	4.4	43 ⁺	0.86	28	
M13	+36	7.7	30.4	0.78	39	5
M3	+28	10.4	26.3	0.55	66	4
M2	-01	11.5	29 ⁺	0.34	120	
M14	-03	9.3	76 ⁺	0.83	54	
Pal 2	+31	27.6	97 ⁺	0.24	209	
M12	-02	4.9	39 ⁺	0.72	10	

Table 3. Name, declination (DEC), distance (d), dispersion measure (DM) observed or ⁺ modeled after Taylor & Cordes (1993), core radius (r_c), collision number (Γ) and number of detected pulsars (N) for the ten highest-ranking candidates for a LOFAR globular cluster survey. Data from Harris (1996) and Freire (2008).

3.3. Pulsars in other galaxies

The next over-dense regions on the sky are galaxies. Their distance is a problem, but compared to globular clusters, galaxies have several advantages for a LOFAR pulsar survey. They are distributed equally over both hemispheres, while most globular clusters are invisible from the telescope site in The Netherlands; and if visible face-on and located in the part of the sky that is pointed away from our Galactic disk, the scatter broadening is relatively low.

In the relatively nearby galaxy M31, a periodicity search based on a 10 hour pointing with the compact core at 140 MHz could detect all pulsars more luminous than ~ 200 Jy kpc² (see eq. 3), which is comparable to the top end of the luminosity distribution in our own galaxy. Any M31 pulsars that emit *giant* pulses (Argyle & Gower 1972) could be discovered more easily through these giant pulses than through their periodicity if the flux ratio between giant and normal pulses exceeds 10^5 (McLaughlin & Cordes 2003). Two young pulsars, the Crab pulsar B0531+21 and LMC pulsar B0540-69 (Staelin & Reifenstein 1968; Johnston & Romani 2003), are known to emit such giant pulses and the former was indeed discovered through them. Compared to the regular periodic emission, giant pulses show a steeper spectral index (-3.0 to -4.5 , Voûte 2001; McLaughlin & Cordes 2003) making giant-pulse searches especially attractive for a low-frequency telescope like LOFAR. Using the McLaughlin & Cordes (2003) maximum distance estimator for giant-pulse detection in 1-hr pointings

$$d = 0.85 \text{ Mpc} \left(\frac{5 \text{ Jy}}{S_{\text{sys}}} \right) \left(\frac{S_{\text{GP}}}{10^5 \text{ Jy}} \right)^{1/2} \left(\frac{B}{10 \text{ MHz}} \right)^{1/4} \quad (5)$$

with $S_{\text{sys}} = G_{\text{core}}/T_{\text{sys}} = (0.8 \times 8.8 \text{ K/Jy})/(1.0 \times 10^3 \text{ K}) = 140 \text{ Jy}$, bandwidth $B = 32 \text{ MHz}$ and scaling the giant pulse flux with spectral index -3.0 , the Crab pulsar would be detectable out to $\sim 1.5 \text{ Mpc}$.

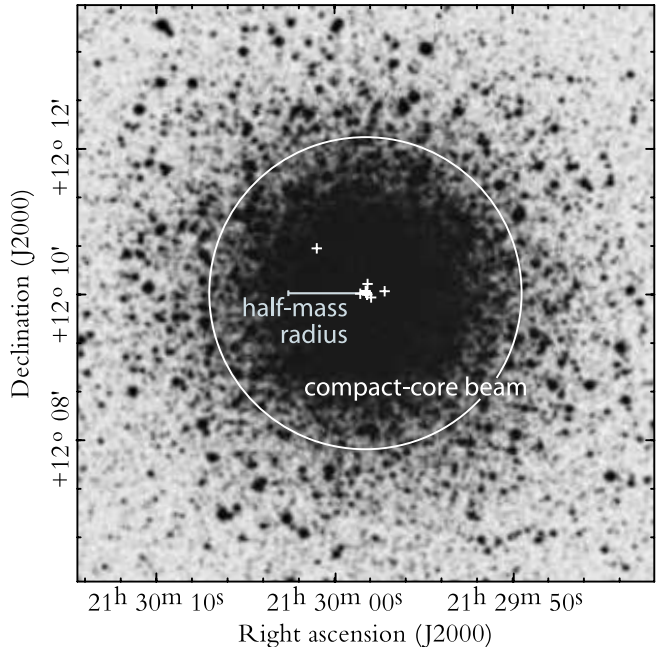


Fig. 7. Beam setup for a MSP survey of M15, the globular cluster with the highest success probability in Table 3. The cluster half-mass radius falls well within the core beam. The crosses mark the 8 pulsars currently known (Anderson 1992).

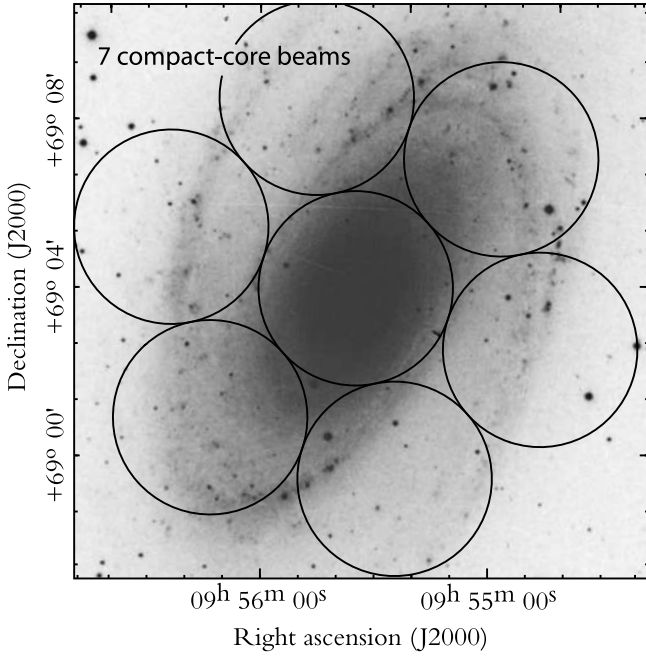


Fig. 8. Seven coherently formed beams from the 2-km LOFAR core projected on candidate galaxy M81 at their FWHM.

Detection of a handful of pulsars in each of several nearby galaxies would enable comparison of the top end of their luminosity functions, and potentially show a relation with galaxy type. Through pulse scattering and dispersion these pulsars will also probe intergalactic matter.

Like for the globular clusters above we have ranked target galaxies by distance, size on the sky and expected number of sources (here assumed to scale linearly with mass). We select galaxies that are within 5 Mpc from the Earth and that are not too strongly scatter broadened given their Galactic latitude gb and inclination angle i (requiring $|gb|+90-i > 30$). In Table 4 we list the 10 highest-ranked candidates. For most of these highest-ranked galaxies the core can be captured with a single compact-core beam (cf. Fig. 8), or the whole galaxy by a pattern of 7 beams.

Name	d Mpc	s arcmin	i deg	gb deg	$\log M$ M_{\odot}
M31	0.7	193	78	-22	11.4
M81	1.4	22	60	41	10.7
M33	0.7	56	56	-31	10.1
M94	4.3	12	33	76	10.8
NGC2403	4.2	23	62	29	10.7
NGC4236	2.2	19	73	47	9.8
NGC4244	3.1	15	90	77	10.0
NGC4395	3.6	13	38	82	10.1
NGC3077	2.1	5	43	42	9.1
UGC7321	3.8	5	90	81	9.7

Table 4. Name, distance (d), size on the sky (s), inclination angle (i), Galactic latitude (gb) and logarithm of the mass ($\log M$) for the ten highest-ranking candidates for a LOFAR extragalactic pulsar survey. Data taken from Tully (1988).

4. Discussion

4.1. Steep spectrum sources

Generally pulsars are increasingly bright toward lower frequencies, but this steep spectrum of pulsars typically flattens out or turns over at a frequency between 100 and 250 MHz (Malofeev et al. 1994). There is, however, a small fraction of pulsars for which no such spectral break is observed down to frequencies as low as 50 MHz. Sources with a spectral index steeper than the spectral index of the sky background of -2.6 (e.g. PSR B0943+10, spectral index -4.0 ; Ramachandran & Deshpande 1994) will be more easily detectable by a telescope like LOFAR, producing quantitative input for radio emission models.

4.2. Follow up

With high sensitivity most important and field of view not a consideration, follow up timing (the determination of pulsar and potential binary parameters, cf. Lorimer & Kramer 2005) will use the entire core, and potentially more of the LOFAR array if it can be reliably phased up, for beam forming. Given the small $3'$ field of view, such follow up needs very accurate candidate source positions. Determining the source position that accurately also directly facilitates timing follow-up by eliminating position as a variable.

In some of the above surveys sources are only localised to within the $30'$ superstation or $5^{\circ}.8$ station beams (cf. Section 3.1.1). Detections can be more accurately located later by following up with many, smaller tied-array beams. As the DM is now known the total computational burden of searching through these many tied-array beams is not as problematic as for an entirely coherent survey. For example, we find that about 50% of incoherent-survey pointings will have sources brighter than the reference S_{min} . Each of these station-beams pointings could subsequently be filled out with 128 coherent superstation beams in about 1/3rd of the original total survey time ($50\% \left(\frac{FoM_{Full}}{FoM_{Superstation}}\right)^2 = 0.36$, cf. Eq. 2 and Table 1) to reach the same S_{min} . This would provide the necessary first conformation observation but also an improved position. In a next step 128 compact-core beams can then similarly tile out the superstation beam in which the source is located to provide full localisation, and the first timing data.

Once sources are properly localised, long-term follow up timing uses tied-array beams. From our simulations we find that in the incoherent reference survey about 80% of sources have nearest neighbors at less than one FWHM station beam away and hence these pairs of sources can be timed simultaneously. 18% and 12% of simulated pulsars are in groups of 3 and 4 per station field-of-view respectively. In total the follow up needs to re-observe about 50% of the survey pointings to time each newly found pulsar once. Sub-arraying or trading bandwidth for independently steerable station beams could potentially increase overall follow-up timing efficiency. The timing observation should hold at least several hundred pulses for a steady profile to form, which at an average $1s$ -pulsar translates to about 10 min integrations. Given the $\sqrt{N_{stations}} = 7.3$ -fold increase in gain between incoherent surveying and tied-array follow-up, a timing run can thus produce high SNR detections for all candidates.

4.3. Fast radio transients

Given the software-telescope nature of LOFAR, piggybacking and simultaneous observing are relatively straightforward to implement. As the 'telescope time' concept at LOFAR includes the availability of central signal processing at CEP, observation modes that are not computationally or IO intensive, such as the incoherent station addition mode, are especially suited for parallel observing. This incoherent mode can therefore run commensally with many of the imaging projects (Röttgering et al. 2006; Fender et al. 2008) to continuously scan a large part of the sky for intermittent pulsars such as PSR B1931+24 (Kramer et al. 2006) and millisecond radio transients (Lorimer et al. 2007; Hessels et al. 2009).

4.4. Survey strategies

Three types of surveys were presented and their overall efficiency (Table 1) is comparable. When deciding which LOFAR survey to implement, considerations relating to the different integration times, beam sizes and operational requirements in these surveys may thus become more important: *Core Coherent* has short (order ~ 1 min) integrations, beneficial for finding accelerated systems and for system stability, and provides good localisation. *Superstation Coherent* and *Full Incoherent* use of order ~ 1 hr integrations, and are well suited for finding intermittent pulsars, but with only reasonable and poor initial localisation respectively. *Core Coherent* and *Superstation Coherent* produce much higher data rates than *Full Incoherent*. Tests on the different types of LOFAR data that are currently becoming available may potentially further differentiate between these strategies.

5. Conclusions

Because of its large area and field of view, LOFAR can reveal the local population of pulsars to a very deep luminosity limit. A 25-day all-sky survey at 140 MHz would find 900 new pulsars, disclosing the local low-luminosity population and roughly doubling the number of pulsars known in the northern hemisphere. Millisecond pulsars in nearby globular clusters can be detected to lower flux limits than previously possible. Assuming the pulsar population in other galaxies is similar to that in ours, we can detect periodicities or giant pulses from extragalactic pulsars up to several Mpc away.

References

Anderson, S. B. 1992, PhD thesis, California Institute of Technology
 Archibald, A. M., Stairs, I. H., Ransom, S. M., et al. 2009, *Science*, 324, 1411
 Argyle, E. & Gower, J. F. R. 1972, *ApJ*, 175, L89
 Arzoumanian, Z., Chernoff, D. F., & Cordes, J. M. 2002, *ApJ*, 568, 289
 Backer, D. C. 1999, in *Perspectives on Radio Astronomy: Science with Large Antenna Arrays*, ed. M. P. van Haarlem
 Bhat, N. D. R., Cordes, J. M., Camilo, F., Nice, D. J., & Lorimer, D. R. 2004, *ApJ*, 605, 759
 Bhattacharya, D., Wijers, R. A. M. J., Hartman, J. W., & Verbunt, F. 1992, *A&A*, 254, 198
 Bower, G. 2007, in *Bulletin of the American Astronomical Society*, Vol. 38, *Bulletin of the American Astronomical Society*, 174+
 Burgay, M., D'Amico, N., Possenti, A., et al. 2003, *Nature*, 426, 531
 Cordes, J. M. 2002, <http://www.astro.cornell.edu/~cordes/documents/aosearch.2002.ps.gz>
 Damashek, M., Taylor, J. H., & Hulse, R. A. 1978, *ApJ*, 225, L31
 Davies, J. G., Lyne, A. G., & Seiradakis, J. H. 1977, *MNRAS*, 179, 635
 Dewey, R. J., Taylor, J. H., Weisberg, J. M., & Stokes, G. H. 1985, *ApJ*, 294, L25
 Fender, R., Wijers, R., Stappers, B., & LOFAR Transients Key Science Project. 2008, ArXiv e-prints

Freire, P. C. 2008, <http://www.naic.edu/~pfreire/GCpsr.html>
 Gunst, A. 2007, private communication
 Harris, W. E. 1996, *AJ*, 112, 1487, updated version at <http://www.physics.mcmaster.ca/resources/globular.html>
 Hartman, J. W. 1997, *A&A*, 322, 127
 Hartman, J. W., Bhattacharya, D., Wijers, R., & Verbunt, F. 1997, *A&A*, 322, 477
 Haslam, C. G. T., Stoffel, H., Salter, C. J., & Wilson, W. E. 1982, *A&AS*, 47, 1
 Hessels, J. W. T., Ransom, S. M., Kaspi, V. M., et al. 2007, ArXiv e-prints, 710
 Hessels, J. W. T., Stappers, B. W., van Leeuwen, J., & LOFAR Transients Key Science Project. 2009, ArXiv e-prints, [arXiv:0903.1447]
 Hewish, A., Bell, S. J., Pilkington, J. D. H., Scott, P. F., & Collins, R. A. 1968, *Nature*, 217, 709
 Hulse, R. A. & Taylor, J. H. 1975, *ApJ*, 201, L55
 Johnston, H. M. & Kulkarni, S. R. 1991, *ApJ*, 368, 504
 Johnston, S. & Romani, R. 2003, *ApJ*, 590, L95
 Johnston, S., Taylor, R., Bailes, M., et al. 2008, *Experimental Astronomy*, 22, 151
 Jonas, J. 2007, in *From Planets to Dark Energy: the Modern Radio Universe*. October 1-5 2007, The University of Manchester, UK. Published online at SISSA, *Proceedings of Science*, p.7
 Kramer, M. 2003, ArXiv Astrophysics e-prints
 Kramer, M., Lyne, A. G., O'Brien, J. T., Jordan, C. A., & Lorimer, D. R. 2006, *Science*, 312, 549
 Kramer, M., Xilouris, K. M., Lorimer, D. R., et al. 1998, *ApJ*, 501, 270
 Lawson, K. D., Mayer, C. J., Osborne, J. L., & Parkinson, M. L. 1987, *MNRAS*
 Lorimer, D. R., Bailes, M., McLaughlin, M. A., Narkevic, D. J., & Crawford, F. 2007, *Science*, 318, 777
 Lorimer, D. R., Faulkner, A. J., Lyne, A. G., et al. 2006, *MNRAS*, 372, 777
 Lorimer, D. R. & Kramer, M. 2005, *Handbook of Pulsar Astronomy* (Cambridge University Press)
 Lyne, A. G., Brinklow, A., Middleditch, J., et al. 1987, *Nature*, 328, 399
 Lyne, A. G. & Lorimer, D. R. 1994, *Nature*, 369, 127
 Lyne, A. G., Manchester, R. N., Lorimer, D. R., et al. 1998, *MNRAS*, 295, 743
 Malofeev, V. M., Gil, J. A., Jessner, A., et al. 1994, *A&A*, 285, 201
 Malofeev, V. M., Malov, O. I., & Shchegoleva, N. V. 2000, *Astronomy Reports*, 44, 436
 Manchester, R. N., Hobbs, G. B., Teoh, A., & Hobbs, M. 2005, *AJ*, 129, 1993
 Manchester, R. N., Lyne, A. G., Camilo, F., et al. 2001, *MNRAS*, 328, 17
 Manchester, R. N., Lyne, A. G., D'Amico, N., et al. 1996, *MNRAS*, 279, 1235
 Manchester, R. N., Lyne, A. G., Taylor, J. H., et al. 1978, *MNRAS*, 185, 409
 McLaughlin, M. A. & Cordes, J. M. 2003, *ApJ*, 596, 982
 Narayan, R. & Ostriker, J. P. 1990, *ApJ*, 352, 222
 Ramachandran, R. & Deshpande, A. A. 1994, *J. Astrophys. Astr.*, 15, 69
 Ramachandran, R., Mitra, D., Deshpande, A. A., McConnell, D. M., & Ables, J. G. 1997, *MNRAS*, 290, 260
 Ransom, S. M., Cordes, J. M., & Eikenberry, S. S. 2003, *ApJ*, 589, 911
 Ransom, S. M., Hessels, J. W. T., Stairs, I. H., et al. 2005, *Science*, 307, 892
 Röttgering, H. 2003, *New Astronomy Review*, 47, 405
 Röttgering, H. J. A., R., B., Barthel, P. D., et al. 2006, in *Cosmology, Galaxy Formation and Astroparticle Physics on the Pathway to the SKA*, ed. H.-R. Klöckner, S. Rawlings, M. Jarvis, & A. Taylor, (<http://www-astro.physics.ox.ac.uk/LOSKA/CONFERENCE/PROCEEDINGS/>)
 Shitov, Y. P. 1994, *Bulletin of the American Astronomical Society*, 26
 Shrauner, J. A., Taylor, J. H., & Woan, G. 1998, *ApJ*, 509, 785
 Smits, R., Kramer, M., Stappers, B., et al. 2009, *A&A*, 493, 1161
 Staelin, D. H. & Reifstein, III, E. C. 1968, *Science*, 162, 1481
 Stappers, B. W., Karappasamy, R., & Hessels, J. W. T. 2008, in *American Institute of Physics Conference Series*, Vol. 983, 40 Years of Pulsars: Millisecond Pulsars, Magnetars and More, ed. C. Bassa, Z. Wang, A. Cumming, & V. M. Kaspi, 593-597
 Stappers, B. W., van Leeuwen, A. G. J., Kramer, M., Stinebring, D., & Hessels, J. 2007, ArXiv Astrophysics e-prints
 Taylor, J. H. & Cordes, J. M. 1993, *ApJ*, 411, 674
 Tully, R. B. 1988, *Nearby galaxies catalog* (Cambridge and New York, Cambridge University Press, 1988, 221 p.)
 van Leeuwen, J. & Verbunt, F. 2004, in *IAU Symposium*, Vol. 218, Young Neutron Stars and Their Environments, ed. F. Camilo & B. M. Gaensler, 41-+
 Verbunt, F. 2003, in *Astronomical Society of the Pacific Conference Series*, Vol. 296, *New Horizons in Globular Cluster Astronomy*, ed. G. Piotto, G. Meylan, S. G. Djorgovski, & M. Riello, 245-+
 Voûte, J. L. L. 2001, PhD thesis, University of Amsterdam
 Wilhelmsson, T. 2007, private communication